Cytotherapy, 2016; 18: 360–370

International Society for Cellular Therapy
ISCT®

CrossMark

Galectin-1 is a local but not systemic immunomodulatory factor in mesenchymal stromal cells

ROBERTA FAJKA-BOJA[1], VERONIKA S. URBÁN[2,3], GÁBOR J. SZEBENI[1], ÁGNES CZIBULA[1], ANDREA BLASKÓ[1], ÉVA KRISTON-PÁL[1], ILDIKÓ MAKRA[1,5], ÁKOS HORNUNG[1,6], ENIKŐ SZABÓ[1], FERENC UHER[3], NÁNDOR G. THAN[4] & ÉVA MONOSTORI[1,*]

[1]Institute of Genetics, Biological Research Centre, Hungarian Academy of Sciences, Szeged, Hungary, [2]Department of Morphology and Physiology, Faculty of Health Sciences, Semmelweis University, Budapest, Hungary, [3]Stem Cell Biology, National Blood Service, Budapest, Hungary, [4]Lendulet Reproduction Research Group, Institute of Enzymology, Research Centre for Natural Sciences, Hungarian Academy of Sciences, Budapest, Hungary, [5]SZTE-MTA Lendület Foldamer Research Group, University of Szeged, H-6720 Szeged, Hungary, and [6]Department of Rheumatology, University of Szeged, Faculty of Medicine, Albert Szent-Györgyi Health Centre, Szeged, Hungary

Abstract

Background aims. Mesenchymal stromal cells (MSCs) have powerful immunosuppressive activity. This function of MSCs is attributed to plethora of the expressed immunosuppressive factors, such as galectin-1 (Gal-1), a pleiotropic lectin with robust anti-inflammatory effect. Nevertheless, whether Gal-1 renders or contributes to the immunosuppressive effect of MSCs has not been clearly established. Therefore, this question was the focus of a complex study. *Methods.* MSCs were isolated from bone marrows of wild-type and Gal-1 knockout mice and their *in vitro* anti-proliferative and apoptosis-inducing effects on activated T cells were examined. The *in vivo* immunosuppressive activity was tested in murine models of type I diabetes and delayed-type hypersensitivity. *Results.* Both Gal-1-expressing and -deficient MSCs inhibited T-cell proliferation. Inhibition of T-cell proliferation by MSCs was mediated by nitric oxide but not PD-L1 or Gal-1. In contrast, MSC-derived Gal-1 triggered apoptosis in activated T cells that were directly coupled to MSCs, representing a low proportion of the T-cell population. Furthermore, absence of Gal-1 in MSCs did not affect their *in vivo* immunosuppressive effect. *Conclusions.* These results serve as evidence that Gal-1 does not play a role in the systemic immunosuppressive effect of MSCs. However, a local contribution of Gal-1 to modulation of T-cell response by direct cell-to-cell interaction cannot be excluded. Notably, this study serves a good model to understand how the specificity of a pleiotropic protein depends on the type and localization of the producing effector cell and its target.

Key Words: *apoptosis, delayed type hypersensitivity, galectin-1, immunosuppression, mesenchymal stromal cells, type I diabetes*

Introduction

Mesenchymal stromal cells (MSCs) represent multipotent adult stem cells. Because of their plasticity in differentiation to mesodermal lineages such as bone, cartilage and adipose tissue and because of their powerful immunosuppressive function [1], MSCs have recently been implicated in various therapeutic approaches [2]. Various immunological pathologies can be efficiently treated by MSC transplantation [3–6], and therefore, the exact nature of their anti-inflammatory function must be correctly defined. Allogeneic and autoimmune/inflammatory responses are dampened [7] by identified soluble and cell-bound factors, such as transforming growth factor (TGF)-β, nitric oxide (NO), indoleamine 2,3-dioxygenase (IDO), prostaglandin E2 (PGE2), hepatocyte growth factor (HGF), human leukocyte antigen (HLA)-G, programmed death ligand 1 (PD-L1) [8,9]; however, the precise role of the individual factors and other mechanisms in the immunosuppressive activity has not yet been suitably clarified.

Recently, the production and secretion of an immunosuppressive factor, galectin-1, has also been identified in MSCs [10–14]. Although Gal-1 has been suggested to contribute to MSCs' immunosuppressive potential [14–16], its true function in their anti-inflammatory activity has been poorly examined.

Correspondence: **Éva Monostori**, PhD, DSc, Institute of Genetics, Biological Research Centre of the Hungarian Academy of Sciences, H-6726 Szeged, Temesvári krt. 62, Hungary. E-mail: monostori.eva@brc.mta.hu

(Received 24 September 2015; accepted 16 December 2015)

ISSN 1465-3249
http://dx.doi.org/10.1016/j.jcyt.2015.12.004

Nevertheless, the immunoregulation by recombinant, soluble Gal-1 has been confirmed in multiple *in vitro* and *in vivo* experimental systems [17]. It has been revealed that Gal-1 reverses the clinical symptoms in animal models of autoimmune and chronic inflammation [18] by various mechanisms, affecting T cells [19], dendritic cells [20], macrophages [21] and extravasation of leucocytes [22]. Gal-1 induces cell death of activated T cells either in soluble [23–25] or in cell-bound form [26], with an increased selectivity toward Th1 and Th17 cells *in vitro* [27], a phenomenon that explains its therapeutic effect in autoimmune inflammatory animal models.

Despite the tremendous *in vitro* and *in vivo* data confirming the immunoregulatory functions of Gal-1, the exact role of Gal-1 in MSCs' immunosuppressive functions has not been thoroughly determined. In this study, we have clearly defined that Gal-1 does not contribute to the systemic immunoregulatory functions of MSCs because the *in vitro* inhibition of T-cell proliferation was not affected by the presence or absence of Gal-1 in MSCs. Moreover, we show that the therapeutic impact of MSCs on autoimmune diabetes and delayed-type hypersensitivity (DTH) in animal models does not depend on their Gal-1 expression. Nevertheless, activated T cells in an intimate cell-to-cell interaction with MSCs undergo apoptosis via a Gal-1-dependent mechanism. Our results may serve an explanation for an important biological problem: how a pleiotropic protein (Gal-1) exerts its specific function (immunosuppression) depending on the type (MSCs) and localization (systemic or tissue) of the producing effector cell and communication with its target (T cells).

Methods

Cells

Bone marrow MSCs were isolated from male C57BL/6 or Gal-1 knockout (strain: B6.Cg-*Lgals1*^{tm1Rob}/J, 006337, Jackson Laboratory) mice as described previously [28]. Briefly, bone marrow cells were collected from femurs and tibias of 8- to 10-week-old male mice and seeded in plastic flask in Dulbecco's Modified Eagle's Medium/Ham's F-12 medium (Invitrogen), complemented with 10% fetal bovine serum (FCS, Invitrogen), 10% horse serum (Invitrogen), 50 U/mL penicillin, 50 µg/mL streptomycin (Sigma-Aldrich), and 2 mmol/L L-glutamine (Invitrogen). Non-adherent cells were removed after 72 h, and then the cell culture medium was changed twice a week. All MSC cultures were free from hematopoietic contamination and used after 10–15 passages. Wild-type and Gal-1-deficient MSCs were designated as wtMSCs and MSC$^{gal1-/-}$, respectively. The cells were cultured in Dulbecco's Modified Eagle's Medium (Gibco, Invitrogen) supplemented with fetal calf serum (10% FCS, Gibco, Invitrogen), penicillin (100 IU/mL), streptomycin (100 µg/mL) and L-glutamine (2 mmol/L) and characterized as described previously [28].

Murine lymphocytes were isolated from the inguinal and mesenteric lymph nodes or the spleen. Homogenized lymphoid tissues were cleared up from erythrocytes by lysis with ammonium-chloride-potassium buffer (150 mmol/L NH_4Cl, 10 mmol/L $KHCO_3$, 0.1 mmol/L ethylenediaminetetraacetic acid). T cells were purified with magnetic bead separation using BD IMag Mouse T Lymphocyte Enrichment Set-DM and BD IMagnet Cell Separation Magnet (BD Biosciences) according to the manufacturer's instructions and were then tested for purity with flow cytometry using anti-CD3 fluorescein isothiocyanate (FITC; BioLegend). The enriched cell population contained 98% of CD3$^+$ T cells (Supplementary Figure S1), which were then cultured in RPMI-1640 (Gibco, Invitrogen) supplemented with FCS (10%), penicillin (100 IU/mL), streptomycin (100 µg/mL), L-glutamine (2 mmol/L) and β-mercaptoethanol (50 µmol/L). All cells were kept in a humidified incubator with 5% CO_2 at 37°C.

Proliferation assay

MSCs were plated into 96-well cell culture plates (Costar, Corning) at different densities and allowed to adhere to the plastic surface. After 3 h, lymph node cell-suspension (2×10^5/well) or enriched T cells (10^5/well) were added to the wells. Lymph node cells and T cells were stimulated in the MSCs/lymphocyte co-cultures for 72 h with 7.5 µg/mL Concanavalin A (Con A) and with Dynabeads Mouse T-activator CD3/CD28 (2 µL beads/well, Invitrogen), respectively. For the thymidine incorporation assay, cells were pulsed with 1 µCi of ^{3}H-thymidine (American Radiolabeled Chemicals) for 16 h before harvesting, and then the incorporated ^{3}H-thymidine was measured with liquid scintillation counter. Alternatively, cell proliferation was measured based on labeling the T cells with CellTrace CFSE Cell Proliferation Kit (2.5 µmol/L, Molecular Probes, Life Technologies) before co-cultures according to the manufacturer's instruction. T cells blocked with mitomycin C (8 µg/mL) served as non-proliferating control cells. Fluorescence intensity of the cellular carboxyfluorescein succinimidyl ester (CFSE) was analyzed with flow cytometry.

MSC-derived factors responsible for the inhibition of T-cell proliferation were analyzed as follows: (i) For the analysis of the anti-proliferative effect of MSC-derived soluble factors, Transwell inserts (pore size 0.4 µm, Costar, Corning) were used in 24-well plates (Costar, Corning). (ii) The inhibition of PD-L1 was carried out by adding neutralizing antibody

(LEAF Purified anti-mouse CD274, BioLegend) or appropriate isotype control (Rat IgG2b κ Isotype Control Functional Grade Purified, eBioscience) to MSCs 1 h before co-cultures. (iii) The NO production was blocked with a competitive inhibitor of NO synthases, N_G-methyl-L-arginine acetate salt (L-NMMA; Sigma-Aldrich), which was used in 50 μmol/L concentration.

Flow cytometry

The CFSE-labeled cells were washed in ice-cold phosphate buffered saline (PBS) supplemented with 1% FCS and 0.1% sodium-azide (fluorescence-activated cell sorting [FACS] buffer). Dead cells were excluded from the analysis with propidium-iodide (10 μg/mL) staining. The cells were then analyzed with FACSCalibur flow cytometer using CellQuest or Modfit software (Becton Dickinson; Supplementary Figure S2). PD-L1 expression of MSCs was triggered with recombinant mouse IFN-γ (20 ng/mL, R&D Systems) treatment for 48 h, then visualized using anti-mouse CD274 (BioLegend) and anti-rat immunoglobulin (Ig)G FITC (Sigma-Aldrich).

Detection of apoptosis

The apoptosis of activated T cells in co-culture with MSCs was examined as described previously [26]. Briefly, MSCs (5×10^3/sample) were plated on round coverslips (12 mm diameter, Menzel Gläser, Thermo Scientific) in 24-well plates. To remove cell surface Gal-1, wtMSCs were treated with 100 mmol/L thiodigalactoside (TDG, Carbosynth) for 30 min at 4°C, and then washed extensively with cell culture medium. Splenocytes (2×10^5 cells/sample) were activated with Con A for 72 h and then labeled with Hoechst 33342 (100 ng/mL for 30 min at 37°C) before co-culturing with MSCs. The cells were co-cultured for 16 h, fixed with 4% paraformaldehyde in PBS for 4 min at room temperature, and then the protein binding sites of the cover slips were saturated in FACS buffer. For the detection of phosphatidylserine exposure on the outer cell membrane, samples were washed with Annexin binding buffer (10 mmol/L 4-(2-hydroxyethyl)-1-piperazineethanesulfonic acid, 140 mmol/L NaCl and 2.5 mmol/L $CaCl_2$) and labeled with Annexin V-Alexa Fluor 488 (Molecular Probes, Life Technologies). For detection of intracellular ceramide release, cells were fixed and permeabilized with permeabilization buffer (PB, FACS-buffer containing 0.1% Triton X-100), and then sequentially incubated with anti-ceramide mAb (Alexis Biochemicals), biotinylated anti-mouse IgM (DAKO) and streptavidin FITC (DAKO). To analyze the depolarization of the mitochondrial membrane, non-fixed samples were loaded with JC-1 dye (Fluka) for 10 min at 37°C and then washed with PBS. The active (cleaved) form of caspase-3 was detected after 24 h of T-cell/MSC co-cultures. Briefly, cells were fixed in 4% paraformaldehyde, permeabilized with PB and treated with rabbit anti-caspase-3 (recognizing the cleaved form, Cell Signaling Technology) and then anti-rabbit IgG-TRITC (DAKO). DNA fragmentation was detected in 24 h co-culture with the DeadEnd Colorimetric TUNEL System (Promega) according the manufacturer's instructions. Finally, the cover slips were mounted with a drop of Fluoromount-G (Southern Biotech).

To determine the apoptosis rate, samples were analyzed with Axioskop 2Mot (Carl Zeiss) fluorescence microscope using AxioCam camera, AxioVision 3.1 software and 20× objective magnification. Image contrast was adjusted using Adobe Photoshop CS4 extended 11.0. In all cases at least 100 cells/samples were analyzed, and the rate of apoptosis was determined as follows: % of apoptotic cells = annexin V positive cells/total cell number × 100.

Quantitative polymerase chain reaction

The tissue culture medium on MSC cell culture was replaced either with conditioned medium harvested from T cells that had been activated via CD3 and CD28 as described earlier or tissue culture medium as control, and then the cells were further cultured for 3 h. Total RNA was extracted from the samples using RNeasy Plus RNA isolation kit (QIAGEN) according to manufacturer's instruction. cDNA was obtained using GoScriptTM Reverse Transcriptase (Promega Corporation) from 2 μg of template total RNA per reaction. To perform quantitative polymerase chain reaction, *Nos2* (Mm01309902_m1) or *Gapdh* (Mm99999915_g1) TaqMan Gene Expression Assays were combined with TaqMan Gene Expression Master Mix (Applied Biosystems) and samples were run in triplicates on Rotor-Gene 3000 instrument (Corbett Life Science). The relative quantification of gene expression was determined by the comparison of threshold values, and all results were normalized to *Gapdh* ($\Delta Ct = Ct_{Gapdh} - Ct_{Nos2}$).

Animal models

All mouse studies were done in strict accordance with national and international laws and regulations of animal experiments and were reviewed and approved by the Institutional Animal Care and Use Committee of the Biological Research Center of the Hungarian Academy of Sciences, and also by the Animal Care and Use Committee of the National Medical Center, Budapest, Hungary.

Streptozotocin-induced type I diabetes model: the induction of diabetes with streptozotocin (STZ) and

the therapy with MSCs and bone marrow hematopoietic progenitor cells were carried out as described previously [29]. Briefly, 8- to 10-week-old female C57BL/6 mice (National Institute of Oncology, Hungary) were injected intraperitoneally with 50 mg/kg of body weight STZ in every 24 h on 5 consecutive days. Blood glucose was measured with an Accu-Chek Active blood glucose meter (F. Hoffmann-La Roche). Those animals were considered diabetic whose blood glucose levels were higher than 10 mmol/L on 2 consecutive days, day 14 and 15 of the experiment. Subsequently, the diabetic mice were sublethally irradiated (250 cGy) and transplanted by tail vein injection with syngeneic bone marrow cells (BMC, 10^6 cells/animal) together with wtMSCs or $MSC^{gal1-/-}$ (10^5 cells/animal). Glucose tolerance test was carried out after overnight fasting, when mice were injected intraperitoneally with 2 g/kg of body weight glucose. Glucose disposal was analyzed by measuring blood glucose at different time points.

DTH model: sensitization of C57BL/6 mice (6–8 weeks old, male) was induced by subcutaneous injection of 100 μg ovalbumin (OVA) emulsified in complete Freund's adjuvant (CFA). The solvent, PBS in CFA, was used as a control. Simultaneously, mice were injected with 10^6 wtMSCs or $MSC^{gal1-/-}$ intraperitoneally. After 4 days, DTH was triggered by injecting 2% heat aggregated OVA into the right hind footpad. The left hind footpad was injected with PBS as a negative control. The thickness of footpads (D) was measured with a precision caliper at time points 0 h and 48 h, and the changes were determined as follows: change in paw diameter = $(D_{right\ 48h} - D_{left\ 48h}) - (D_{right\ 0h} - D_{left\ 0h})$.

Statistical analyses

Mean and SD were determined with Microsoft EXCEL software from the results of at least three independent experiments, each conducted in duplicate or triplicate samples, unless indicated otherwise in the figure legends. Statistical analysis was performed using one-way analysis of variance test (ANOVA) in GraphPad Prism Version 6.03. When significant by ANOVA ($P < 0.05$), pairwise comparisons of experimental groups were carried out using Fisher's least-significant difference (LSD) method as a *post hoc* test (set at $^*P < 0.05$, $^{**}P < 0.01$, $^{***}P < 0.001$).

Results

MSCs from wild-type and Gal-1 knockout mice similarly affect T-cell proliferation

To investigate the precise function of Gal-1 in the immunomodulatory effect of MSCs, we compared MSCs isolated from the bone marrow of wild-type or Gal-1 knockout mice. The detailed characterization regarding the expression of Gal-1, cell surface markers and differentiation potential of wtMSCs and $MSC^{gal1-/-}$ was previously described [28]. The optimal MSC/T-cell ratio was determined to be 1:10 (Supplementary Figure S3), which was then used in all co-culture experiments. Both wtMSCs and $MSC^{gal1-/-}$ inhibited similarly the proliferation of Con A activated lymph node T cells (Figure 1A) or purified T cells stimulated with CD3/CD28 mAbs (Figure 1B).

Proximity of MSCs and T cells is compulsory for the inhibition of T-cell proliferation

The immunosuppressive effect of MSCs is based on the expression of multiple soluble (such as TGF-β, NO, IDO, PGE2, HGF, HLA-G) and cell-bound factors (PD-L1). To examine the requirement of the proximity between MSC and T cells for the inhibition of T-cell proliferation by MSCs, we cultured MSCs and purified T cells either in direct co-cultures or separated in Transwell inserts (Figure 2). When MSCs and T cells were sequestered by a membrane, the anti-proliferative effect of both wtMSC and $MSC^{gal1-/-}$ were diminished (Figure 2), suggesting the necessity of close proximity of target (T cells) and effector (MSCs) cells.

The contribution of Gal-1 in MSC-mediated inhibition of T-cell proliferation could be excluded due to the similar anti-proliferative effect of wtMSC and MSC^{gal-1} (Figures 1 and 2). Therefore, the potential role of another MSC cell surface protein, PD-L1 (CD274, B7-H1), which acts in direct cell-to-cell contact [30], was examined. Cell surface PD-L1 was not detected on resting MSCs, but it was expressed on stimulation with an inflammatory cytokine, interferon (IFN0-γ; Figure 3A). Because a neutralizing antibody against PD-L1 did not influence the inhibitory effect of IFN-γ-treated MSCs on T-cell proliferation (Figure 3B), the regulatory function of PD-L1 could be ruled out.

We then examined another anti-proliferative messenger produced by murine MSCs, NO [31], which is considered a short-lived, highly reactive compound, diffusing away only 100–200 μm from the producing cell [32]. Of note, supernatants harvested from activated T cells induced *Nos2* gene expression in both wtMSC and $MSC^{gal1-/-}$ (Figure 3C). The inhibitor of NO synthesis, L-NMMA, decreased the anti-proliferative effect of MSCs regardless of their Gal-1 expression (Figure 3D), suggesting an important role of NO in the immunosuppressive effect.

MSC-derived Gal-1 triggers apoptosis of activated T cells in direct cell-to-cell contact

It has been substantially verified that Gal-1 induces apoptosis of activated T cells, either in soluble form [23,24] or in direct cell-to-cell contact with

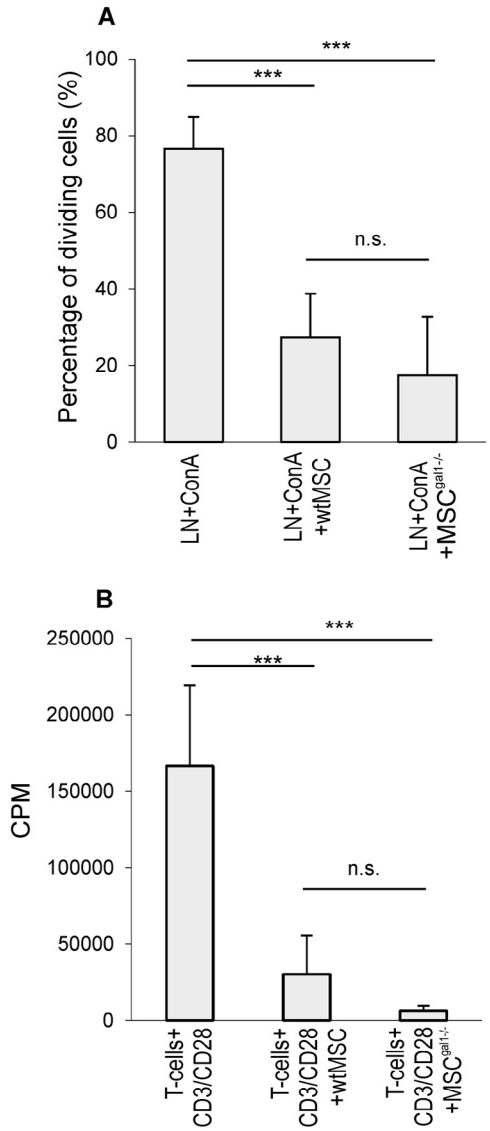

Figure 1. MSC-derived Gal-1 does not play a role in the inhibition of T-cell proliferation by MSCs. (A) CFSE-labeled lymph node (LN) cells were activated with Con A in the presence or absence of wtMSCs or MSC$^{gal1-/-}$ for 72 h and were then analyzed with flow cytometry. Bars show mean ± SD of data pooled from three independent experiments, each conducted in triplicates. (B) Purified T cells were activated with anti-CD3/CD28 beads in the presence or absence of wtMSCs or MSC$^{gal1-/-}$ for 72 h. Cells were pulsed with 1 μCi of ^{3}H-thymidine for the last 16 h of activation, and then the incorporation of ^{3}H-thymidine was measured. Bars show mean ± SD of data pooled from seven independent experiments, each conducted in triplicates. Statistics: ANOVA ($P < 0.05$), followed by Fisher's least significant difference method, ***$P < 0.001$, n.s., not significant; CPM, counts per minute.

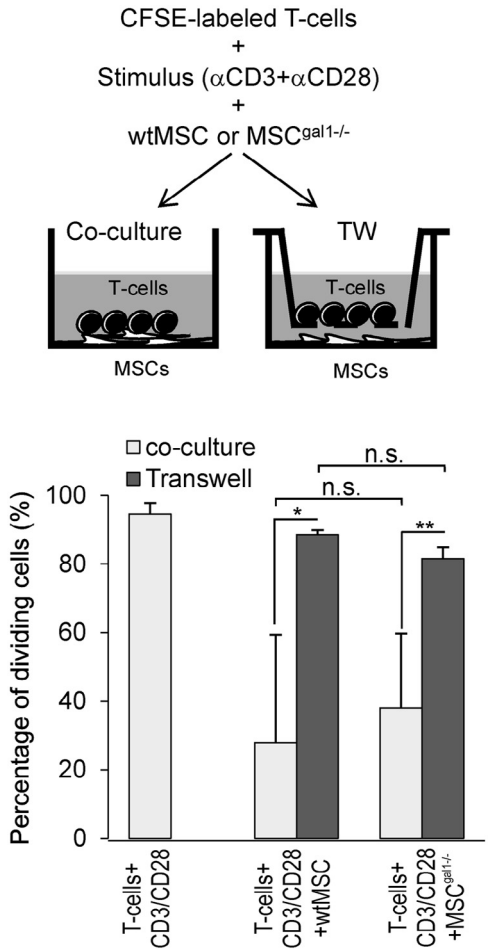

Figure 2. MSCs require direct co-culture with T cells for their antiproliferative effect. CFSE-labeled T cells were activated with anti-CD3/CD28 beads and were then co-cultured with wtMSCs or MSC$^{gal1-/-}$ in direct co-cultures (gray bars) or in indirect co-cultures physically separated by a Transwell insert (TW, dark bars). See experimental scheme (upper panel). CFSE fluorescence intensity of the samples was analyzed with flow cytometry after 72 h. The percentage of proliferating T cells in the various culture conditions is presented as mean ± SD of data pooled from three independent experiments. Statistics: ANOVA ($P < 0.05$), followed by Fisher's least significant difference method, *$P < 0.05$, **$P < 0.01$, n.s., not significant.

Gal-1-secreting effector cells [26]. Indeed, mouse MSCs induced the apoptosis of activated T cells in a Gal-1-dependent fashion because wtMSCs but not MSC$^{gal1-/-}$ triggered T-cell death (Figure 4). The mechanism of T-cell apoptosis was similar to that of human-activated T cells induced by Gal-1 expressing human tumor cells in co-culture [26] or by soluble recombinant Gal-1 [24]. This was characterized by the extracellularly exposed phosphatidylserine (Figure 4A), ceramide release (Figure 4B), decreased mitochondrial membrane potential (Figure 4*C*), caspase activation (Figure 4D) and DNA fragmentation (Figure 4E). All of these events were diminished with Gal-1 deficiency in MSC$^{gal1-/-}$ (Figure 4A–E) or with the presence of Gal-1 inhibitor TDG, a lactose analogue that competes with cell surface glycoconjugates (Figure 4A). Apoptosis was strictly dependent on direct MSC–T-cell contact because it was only detected with fluorescence microscopy on MSC-coupled T cells,

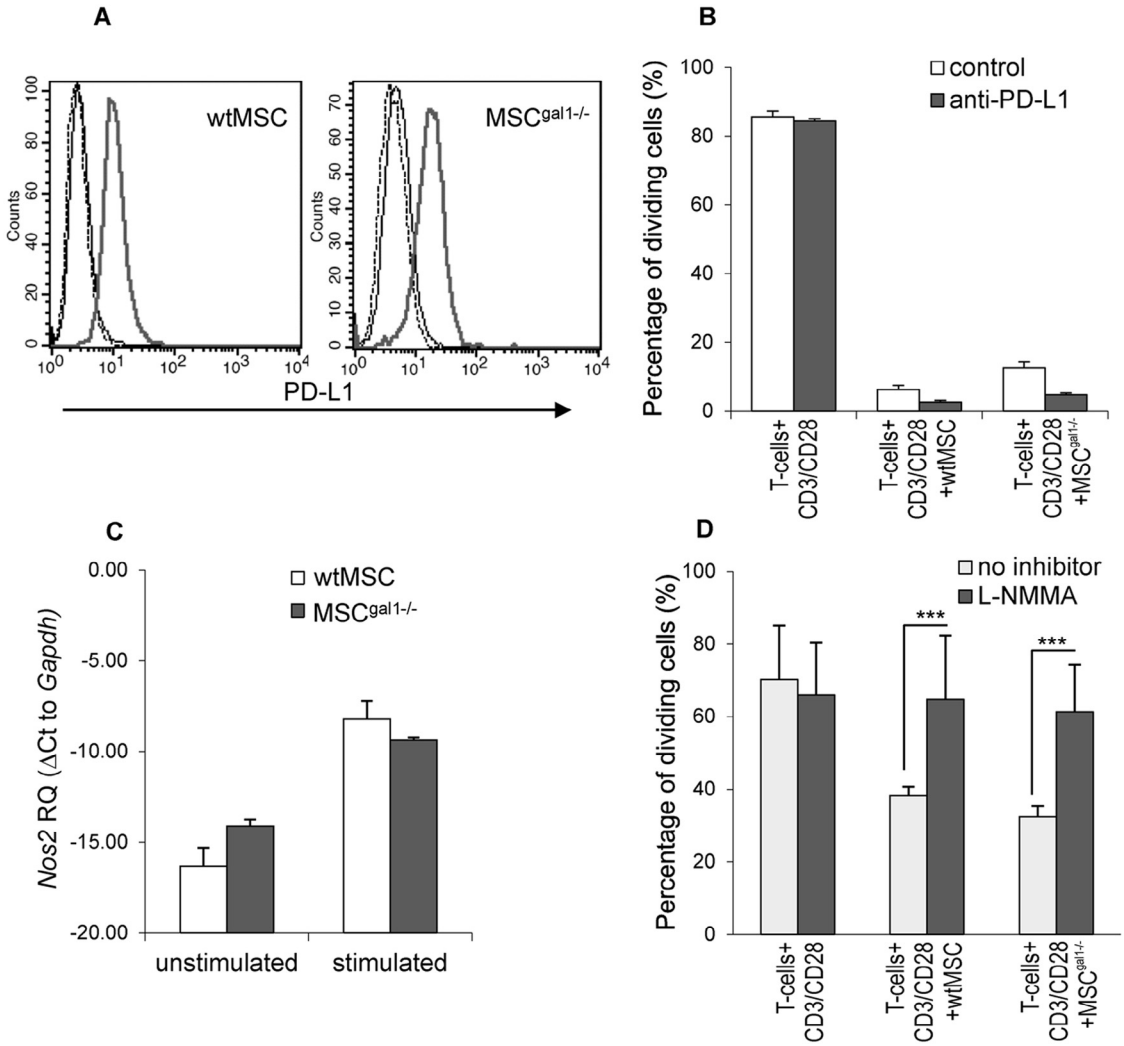

Figure 3. Nitric oxide synthase and its product NO, but not PD-L1, contribute to the immunosuppressive effect of wtMSCs or MSC$^{gal1-/-}$. (A) PD-L1 expression of wtMSC (left panel) and MSC$^{gal1-/-}$ (right panel) was triggered with recombinant mouse IFN-γ (20 ng/mL) for 48 h, and then visualized using anti-mouse CD274 and anti-rat IgG FITC. Dashed line: isotype control antibody; black line: PD-L1 expression of unstimulated MSCs; gray line: PD-L1 expression of IFN-γ-stimulated MSCs. (B) MSCs were pre-treated with neutralizing PD-L1 (dark bars) or isotype matched antibody (control, white bars) for 1 h and then co-cultured with CFSE-labeled T cells in the presence of anti-CD3/CD28 beads. CFSE fluorescence intensity was analyzed with flow cytometry after 48 h. The mean ± SD of the percentage of cells with decreased CFSE is presented, pooled from two independent experiments, each conducted in triplicates. (C) Supernatants from activated T cells were added to wtMSCs (white bars) or MSC$^{gal1-/-}$ (dark bars) for 3 h, or both of these cells were left unstimulated. Relative quantity (RQ) of *Nos2* mRNA compared with *Gapdh* mRNA was detected with quantitative polymerase chain reaction ($\Delta Ct = Ct_{Gapdh} - Ct_{Nos2}$). Mean ± SD of data from three independent experiments are shown. (D) CFSE-labeled T cells were activated with anti-CD3/CD28 beads in the absence or presence of wtMSCs or MSC$^{gal1-/-}$ with (gray bars) or without (white bars) Nos2 inhibitor, L-NMMA, and then analyzed with flow cytometry. The percentage of cells with decreased CFSE fluorescence intensity represent dividing cells, presented on the graph as mean ± SD of the data pooled from two independent experiments, each conducted in triplicates. Statistics: ANOVA ($P < 0.05$), followed by Fisher's least significant difference method, ***$P < 0.001$.

whereas the overall apoptosis rate in the whole T-cell population in co-culture could not be confirmed by cytofluorometry (data not shown).

MSC derived Gal-1 does not play a role in MSCs' immunosuppressive effects in vivo

As our *in vitro* results showed, MSC-derived Gal-1 was an effective apoptosis-inducing factor for activated T cells in direct cell-to-cell contact. On the other hand, Gal-1 deficiency in MSCs did not affect the proliferation inhibition of T cells in the co-culture. Whether Gal-1 played a role in the systemic immunosuppressive effects of MSCs *in vivo* remained a relevant question because many studies have reported an immunosuppressive and therapeutic effect of either MSCs [33] or soluble Gal-1 [17,18] in autoimmune and chronic inflammatory diseases.

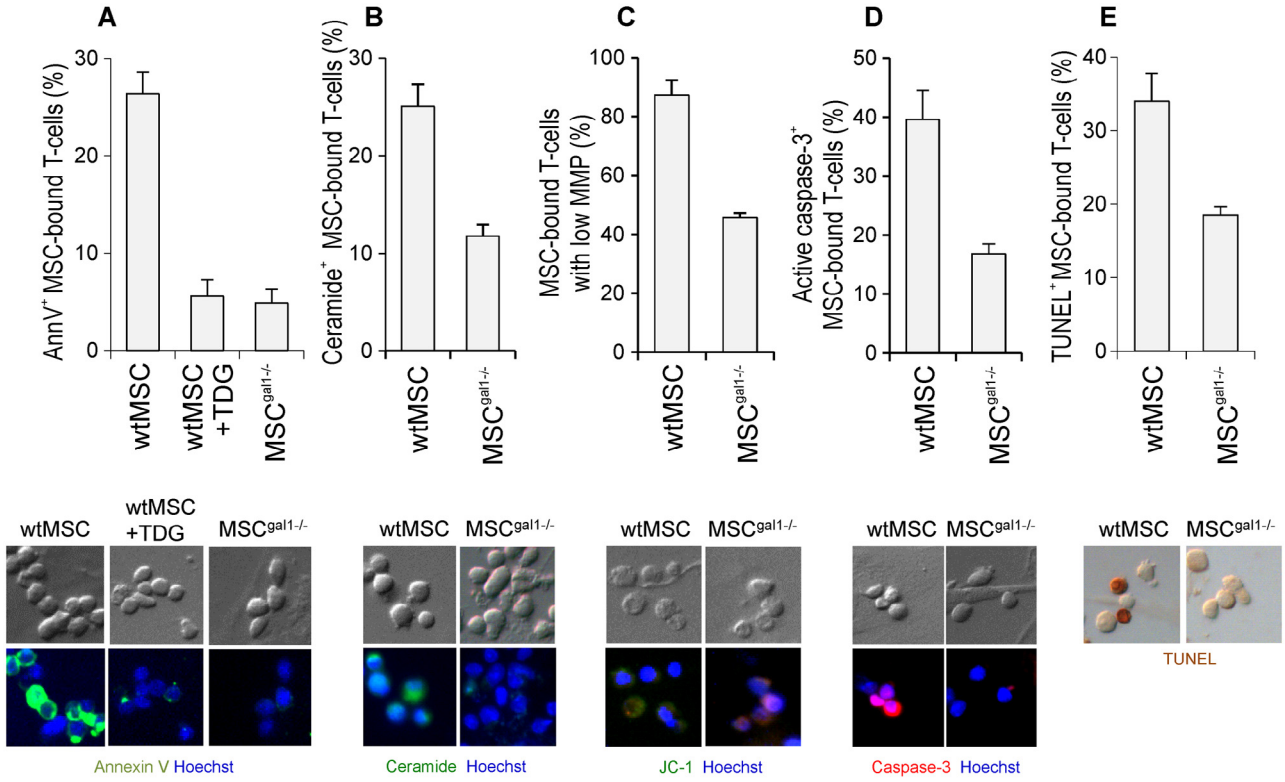

Figure 4. MSC-derived Gal-1 induces apoptosis of activated T cells. T cells were activated with 7.5 μg/mL Con A for 72 h, and then the nuclei were labeled with Hoechst 33342 (blue). Activated T cells were then co-cultured with wtMSCs or MSC$^{gal1-/-}$ for 16 h (A–C) or 24 h (D, E). (A) The cells were fixed, stained with Annexin V-Alexa Fluor 488 (green) and analyzed with fluorescence microscope. For removal of cell-surface Gal-1, wtMSCs were pre-incubated with TDG before co-cultures. (B) Detection of ceramide levels was carried out by incubating the samples with anti-ceramide mAb and then with biotinylated anti-mouse IgM and streptavidin-FITC (green). (C). Changes in the mitochondrial membrane potential (MMP) (red: high MMP, green: low MMP) was detected with JC-1 fluorescence dye labeling. (D) Caspase-3 activation was visualized with anti-cleaved caspase-3 antibody and anti-rabbit IgG-TRITC (red). (E) DNA fragmentation was observed with terminal deoxynucleotidyl transferase dUTP nick-end labeling (TUNEL) assay (brown). Samples were analyzed with fluorescence and light microscopy. Scale bar represents 10 μm. The bars show mean ± SD of the percentage of positive cells, counted from at least 100 cells in 5 non-overlapping fields of view and two independent experiments.

Therefore, the therapeutic effects of wtMSCs or MSC$^{gal1-/-}$ was examined in two experimental immunological disorders, type I diabetes and DTH. In a previous study, we showed that wtMSCs had therapeutic effects on STZ-induced diabetic mice and suppressed the T-cell-mediated immune response against newly formed pancreatic β-islet cells [29]. The function of wild-type and Gal-1-deficient MSCs were compared in the preceding model (Figure 5A). Both wtMSCs and MSC$^{gal1-/-}$ successfully increased the survival of STZ-treated mice (Figure 5B) and restored the blood glucose level to normal values (Figure 5C), suggesting that MSCs' immunosuppressive effect was not dependent on their Gal-1 production.

Next, we tested the role of MSC-derived Gal-1 in a DTH mouse model, induced by OVA, because wtMSCs were described as potent inhibitors of paw edema in a recent study [31]. Wild-type or Gal-1-deficient MSCs were injected at the time of OVA sensitization (Figure 6A). Both wtMSCs and MSC$^{gal1-/-}$ significantly diminished the OVA-induced paw edema in hind limbs (Figure 6B), indicating that the inhibition of DTH reaction by MSCs was independent of their Gal-1 production.

Discussion

MSCs express a plethora of immunosuppressive factors; hence, these cells are considered potential therapeutic tools in immune disorders. One of these potent anti-inflammatory factors is galectin-1, which is abundantly expressed in MSCs as shown by transcriptomic and proteomic approaches [10,11]. Although Gal-1 in MSCs has been implicated in inhibitory effects on T-cell proliferation [14–16], the role of Gal-1 in MSCs from an immunoregulatory point of view has not yet been precisely clarified. The *in vitro* studies that have examined this issue used various methods: inhibition of Gal-1 with thiodigalactoside, which blocks Gal-1 binding to carbohydrate ligands [14], blocking of Gal-1 with specific antibodies [15] and generation of stable Gal-1 knockdown in MSC clones [16]. All of these methods

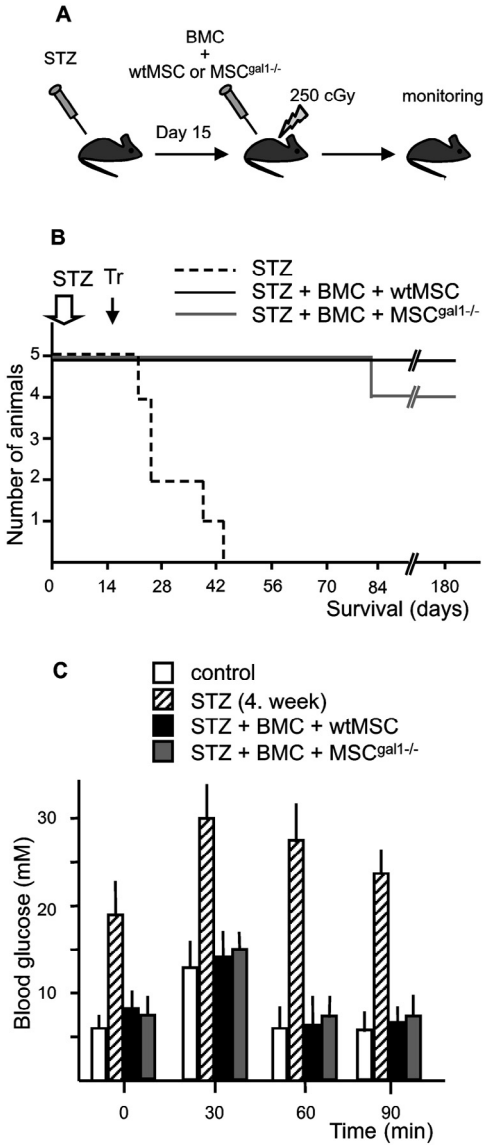

Figure 5. Galectin-1 expression does not play a role in the therapeutic effects of MSCs on STZ-induced diabetes. (A) Type I diabetes was induced in C57BL/6 mice by serial low-dose injection of STZ. On day 15, mice were irradiated with dose of 250 cGy and then transplanted with syngeneic BMCs (10^6 cells/animal) and wtMSCs or MSC$^{gal1-/-}$ (10^5 MSCs/animal). n = 5/group. (B) Survival of diabetic mice treated with BMCs and wtMSCs (black line) or MSC$^{gal1-/-}$ (gray line), or untreated (dashed line) was followed up to 180 days. (C) Glucose tolerance test was carried out with mice fasting overnight and then injected with 2 g/kg of body weight glucose intraperitoneally. Blood sugar levels of control mice (white bars), STZ-induced diabetic mice (striped bars), diabetic mice treated with BMCs and wtMSCs (black bars) or MSC$^{gal1-/-}$ (gray bars) were measured at the indicated time points after glucose loading.

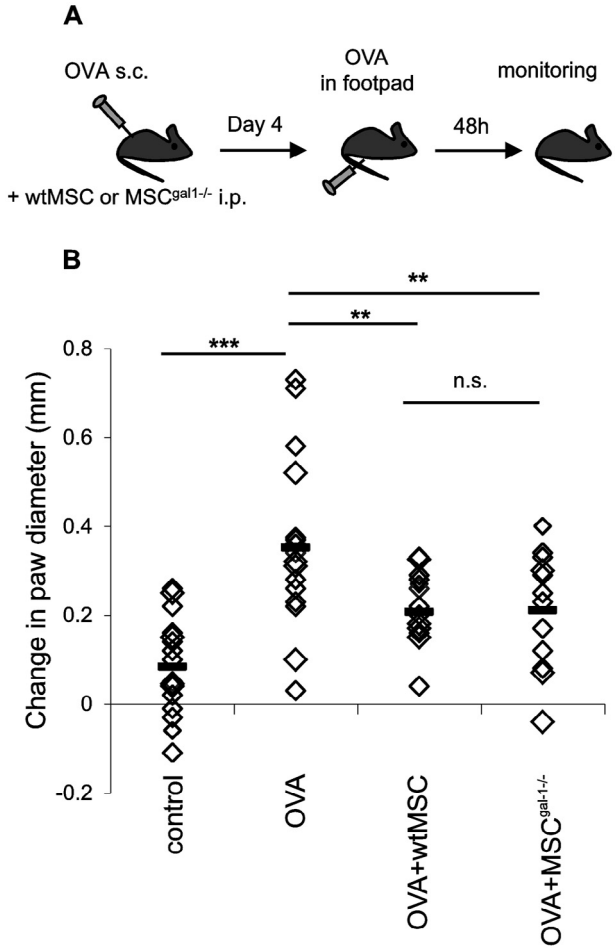

Figure 6. MSCs inhibit delayed-type hypersensitivity in a Gal-1 independent fashion. (A) Mice (C57BL/6) were sensitized with subcutaneous OVA injection or received PBS as control. At the same time point, mice were injected with wtMSCs, MSC$^{gal1-/-}$ or PBS intraperitoneally. Four days later, the DTH reaction was triggered by injecting heat-aggregated OVA into the right hind limb, and the left hind limb was injected with PBS. (B) Paw edema was followed by measuring the diameter of hind limbs 48 h after triggering DTH. The change in the paw diameter was calculated as described in the Methods section. Bars are drawn to the means, and each square is a single replicate. n = 14–15. Statistics: ANOVA ($P < 0.05$), followed by Fisher's least significant difference method, $^{**}P < 0.01$, $^{***}P < 0.001$, n.s., not significant.

have their drawbacks: thiodigalactoside does not react solely with Gal-1 but may interact with other lectins as well, and blocking antibodies may only be partially effective [14,15]. Furthermore, the generation of stable galectin-1 knockdown MSC clones [16] bears the possibility for off-target effect of the knockdown construct and also raises the problem of generating less potent MSC clones from the substantially heterogenic MSC population, irrespective of their Gal-1 expression [34]. To avoid these disadvantages, we used wild-type and Gal-1-deficient MSCs isolated from wild-type and Gal-1 knockout mice, respectively. Both wtMSCs and MSC$^{gal1-/-}$ display the same characteristics including cell surface markers, differentiation capacity [28] and expression of the main immunosuppressive genes, *Nos2*, *Cox2* and *Tgfβ* (Figure 3; see also Augello et al.) [30]. Despite its Gal-1 deficiency, MSC$^{gal1-/-}$ is as effective in the inhibition of T-cell proliferation as the wild-type MSCs (Figure 1). Furthermore, both wild-type

and Gal-1 knockout MSCs upregulate their *Nos2* expression in response to inflammatory cytokines produced by activated T cells, and the Nos2 inhibitor L-NMMA reverts the proliferation to the level of T cells without MSCs (Figure 3). These results show that NO, a messenger which acts at short distances but does not require direct cell interaction between the effector and target cells, mediates proliferation inhibition. In contrast, Gal-1 acting via intimate cell-to-cell contact [26,35] on activated T cells is not able to modify cell growth at low MSC/T-cell ratio (such as 1:10), where only a small portion of T cells are activated at the beginning of co-culture and liaise strong interaction with the stromal cells, whereas the majority of the T cells do not attach directly to the MSCs.

While MSC-produced Gal-1 is not involved in MSC-mediated inhibition of Con A induced proliferation, apoptosis induction of activated T cells depends on MSC-produced Gal-1 (Figure 4). These apparently controversial activities of Gal-1 are explained by two facts: (i) cell-bound Gal-1 triggers apoptosis only on those T cells that are activated (aT-cells) and directly couple to the Gal-1 expressing effector cells (MSCs). The MSC-coupled aT-cells represent only a small fraction of all target cells in the co-culture; therefore, significant Gal-1-dependent T-cell death in the entire T-cell population cannot be detected. (ii) An assay of T-cell proliferation represents a different experimental condition because resting T cells are activated in the presence of MSCs. Therefore, the proliferation is stimulated in the presence of the inhibitory cellular component (MSC) whereas apoptosis occurs only on those T cells that are already activated and have intimate interaction with MSCs. The latter can be a rare event at the cell population level under the conditions of the proliferation experiment. The molecular mechanism (Figure 4) of the apoptosis is identical to that previously described by our laboratory for recombinant or tumor cell–derived Gal-1 [25,26].

Our *in vitro* studies resulted in an important conclusion: Gal-1 in MSCs does not contribute to the immunosuppressive function of MSCs unless MSCs and T cells in an activated state come into close and intimate contact. To extend and validate these results, Gal-1 dependence of the *in vivo* immunosuppressive potential of MSCs has been analyzed in two mouse models, OVA-induced DTH [31] and STZ-induced type I diabetes [29], in which the therapeutic effect of wild-type MSCs has been previously reported. Supporting the *in vitro* results, both wtMSCs and $MSC^{gal1-/-}$ successfully reduced the OVA-induced paw edema in a DTH model (Figure 6) and healed STZ-induced type I diabetes (Figure 5) irrespective of the Gal-1 expression by MSCs. The experiments presented here support our theory that Gal-1 does not participate in the systemic immunosuppressive function of MSCs; however, it may fulfill its immunoregulatory role locally when direct cell-to-cell interaction between MSCs and T cells occurs.

There is no doubt that Gal-1 exerts an immunosuppressive function under certain circumstances. The cellular delivery of Gal-1 by Gal-1 transgenic dendritic cells (Gal-1tgDC) results in a therapeutic effect on diabetes in NOD mice [36]. Perone et al. [36] clearly showed that dendritic cells (DCs) localize in the lymph nodes and spleen, the sites of immune responses, and Gal-1 in DCs operates as a pro-apoptotic factor on activated antigen-specific T cells. In this situation, the antigen-presenting DCs and the antigen-specific T cells establish a close interaction, resulting in Gal-1tgDC-induced T-cell apoptosis in a Gal-1-dependent fashion. In contrast, MSCs used as therapeutic means in diabetes model do not localize in the immune organs or in the damaged pancreas in the diabetic animals [29], indicating that their role in tissue regeneration is accounted for an indirect rather than a local effect. Indeed, a recent study suggested that MSCs polarized tissue-resident macrophages, microglia cells, into an immunosuppressive M2 phenotype, rendering MSCs' anti-inflammatory function an indirect and long-term effect [37]. We have recently demonstrated another function of MSC-derived Gal-1 in solid tumors, where MSCs resided within the tumor tissue and promoted angiogenesis and thus tumor growth in a Gal-1–dependent fashion, but they did not contribute to the tumor immuno-privilege [28]. Thus, as we show here, the immunosuppressive function of MSCs does not rely on their Gal-1 expression because Gal-1 can function only in direct cell-to-cell contact.

Our results may serve a useful model to explain an important biological problem: how a pleiotropic protein (Gal-1) exerts its specific function (immunosuppression) depending on the type (MSCs) and localization (systemic or tissue) of the producing effector cell and communication with its target (T cells).

Acknowledgments

The authors thank Mrs. Andrea Gercsó for her excellent technical assistance and Edit Kotogány for flow cytometric analysis. This work was supported by the Hungarian Scientific Research Fund (OTKA PD75938, principal investigator: R.F.B.). R.F.B. has been supported by János Bolyai Research Fellowship of the Hungarian Academy of Sciences. Publication fee of the manuscript was supported by the Hungarian Academy of Sciences Lendulet Grant LP2014-7/2014 (Principal investigator, N.G.T.)

Disclosure of interest: The authors have no commercial, proprietary, or financial interest in the products or companies described in this article.

References

[1] Ma S, Xie N, Li W, Yuan B, Shi Y, Wang Y. Immunobiology of mesenchymal stem cells. Cell Death Differ 2014;21:216–25.

[2] Ankrum J, Karp JM. Mesenchymal stem cell therapy: two steps forward, one step back. Trends Mol Med 2010;16:203–9.

[3] Ringden O, Le Blanc K. Mesenchymal stem cells for treatment of acute and chronic graft-versus-host disease, tissue toxicity and hemorrhages. Best Pract Res Clin Haematol 2011;24:65–72.

[4] Wang D, Zhang H, Liang J, Li X, Feng X, Wang H, et al. Allogeneic mesenchymal stem cell transplantation in severe and refractory systemic lupus erythematosus: 4 years of experience. Cell Transplant 2013;22:2267–77.

[5] Carlsson PO, Schwarcz E, Korsgren O, Le Blanc K. Preserved β-cell function in type 1 diabetes by mesenchymal stromal cells. Diabetes 2015;64:587–92.

[6] Voswinkel J, Francois S, Simon JM, Benderitter M, Gorin NC, et al. Use of mesenchymal stem cells (MSC) in chronic inflammatory fistulizing and fibrotic diseases: a comprehensive review. Clin Rev Allergy Immunol 2013;45:180–92.

[7] Le Blanc K, Tammik L, Sundberg B, Haynesworth SE, Ringdén O. Mesenchymal stem cells inhibit and stimulate mixed lymphocyte cultures and mitogenic responses independently of the major histocompatibility complex. Scand J Immunol 2003;57:11–20.

[8] Shi Y, Su J, Roberts AI, Shou P, Rabson AB, Ren G. How mesenchymal stem cells interact with tissue immune responses. Trends Immunol 2012;33:136–43.

[9] Hegyi B, Kudlik G, Monostori E, Uher F. Activated T-cells and pro-inflammatory cytokines differentially regulate prostaglandin E2 secretion by mesenchymal stem cells. Biochem Biophys Res Commun 2012;419:215–20.

[10] Silva WA Jr, Covas DT, Panepucci RA, Proto-Siqueira R, Siufi JL, Zanette DL, et al. The profile of gene expression of human marrow mesenchymal stem cells. Stem Cells 2003;21:661–9.

[11] Kadri T, Lataillade JJ, Doucet C, Marie A, Ernou I, Bourin P, et al. Proteomic study of Galectin-1 expression in human mesenchymal stem cells. Stem Cells Dev 2005;14:204–12.

[12] Phinney DG, Hill K, Michelson C, DuTreil M, Hughes C, Humphries S, et al. Biological activities encoded by the murine mesenchymal stem cell transcriptome provide a basis for their developmental potential and broad therapeutic efficacy. Stem Cells 2006;24:186–98.

[13] Pedemonte E, Benvenuto F, Casazza S, Mancardi G, Oksenberg JR, Uccelli A, et al. The molecular signature of therapeutic mesenchymal stem cells exposes the architecture of the hematopoietic stem cell niche synapse. BMC Genomics 2007;8:65–78.

[14] Najar M, Raicevic G, Id Boufker H, Stamatopoulos B, De Bruyn C, Meuleman N, et al. Modulated expression of adhesion molecules and galectin-1: role during mesenchymal stromal cell immunoregulatory functions. Exp Hematol 2010;38:922–32.

[15] Lepelletier Y, Lecourt S, Renand A, Arnulf B, Vanneaux V, Fermand JP, et al. Galectin-1 and semaphorin-3A are two soluble factors conferring T-cell immunosuppression to bone marrow mesenchymal stem cell. Stem Cells Dev 2010;19:1075–9.

[16] Gieseke F, Böhringer J, Bussolari R, Dominici M, Handgretinger R, Müller I. Human multipotent mesenchymal stromal cells use galectin-1 to inhibit immune effector cells. Blood 2010;116:3770–9.

[17] Camby I, Le Mercier M, Lefranc F, Kiss R. Galectin-1: a small protein with major functions. Glycobiology 2006;16:137R–57.

[18] Rabinovich GA, Toscano MA. Turning 'sweet' on immunity: galectin-glycan interactions in immune tolerance and inflammation. Nat Rev Immunol 2009;9:338–52.

[19] Toscano MA, Commodaro AG, Ilarregui JM, Bianco GA, Liberman A, Serra HM, et al. Galectin-1 suppresses autoimmune retinal disease by promoting concomitant Th2- and T regulatory-mediated anti-inflammatory responses. J Immunol 2006;176:6323–32.

[20] Ilarregui JM, Croci DO, Bianco GA, Toscano MA, Salatino M, Vermeulen ME, et al. Tolerogenic signals delivered by dendritic cells to T cells through a galectin-1-driven immunoregulatory circuit involving interleukin 27 and interleukin 10. Nat Immunol 2009;10:981–91.

[21] Barrionuevo P, Beigier-Bompadre M, Ilarregui JM, Toscano MA, Bianco GA, Isturiz MA, et al. A novel function for galectin-1 at the crossroad of innate and adaptive immunity: galectin-1 regulates monocyte/macrophage physiology through a nonapoptotic ERK-dependent pathway. J Immunol 2007;178:436–45.

[22] Norling LV, Sampaio AL, Cooper D, Perretti M. Inhibitory control of endothelial galectin-1 on in vitro and in vivo lymphocyte trafficking. FASEB J 2008;22:682–90.

[23] Perillo NL, Pace KE, Seilhamer JJ, Baum LG. Apoptosis of T cells mediated by galectin-1. Nature 1995;378:736–9.

[24] Ion G, Fajka-Boja R, Kovács F, Szebeni G, Gombos I, Czibula Á, et al. Acid sphingomyelinase mediated release of ceramide is essential to trigger the mitochondrial pathway of apoptosis by galectin-1. Cell Signal 2006;18:1887–96.

[25] Blaskó A, Fajka-Boja R, Ion G, Monostori E. How does it act when soluble? Critical evaluation of mechanism of galectin-1 induced T-cell apoptosis. Acta Biol Hung 2011;62:106–11.

[26] Kovács-Sólyom F, Blaskó A, Fajka-Boja R, Katona RL, Végh L, Novák J, et al. Mechanism of tumor cell-induced T-cell apoptosis mediated by galectin-1. Immunol Lett 2010;127:108–18.

[27] Toscano MA, Bianco GA, Ilarregui JM, Croci DO, Correale J, Hernandez JD, et al. Differential glycosylation of TH1, TH2 and TH-17 effector cells selectively regulates susceptibility to cell death. Nat Immunol 2007;8:825–34.

[28] Szebeni GJ, Kriston-Pál É, Blazsó P, Katona RL, Novák J, Szabó E, et al. Identification of galectin-1 as a critical factor in function of mouse mesenchymal stromal cell-mediated tumor promotion. PLoS ONE 2012;7(7):e41372.

[29] Urbán VS, Kiss J, Kovács J, Gócza E, Vas V, Monostori E, et al. Mesenchymal stem cells cooperate with bone marrow cells in therapy of diabetes. Stem Cells 2008;26:244–53.

[30] Augello A, Tasso R, Negrini SM, Amateis A, Indiveri F, Cancedda R, et al. Bone marrow mesenchymal progenitor cells inhibit lymphocyte proliferation by activation of the programmed death 1 pathway. Eur J Immunol 2005;35:1482–90.

[31] Ren G, Zhang L, Zhao X, Xu G, Zhang Y, Roberts AI, et al. Mesenchymal stem cell-mediated immunosuppression occurs via concerted action of chemokines and nitric oxide. Cell Stem Cell 2008;2:141–50.

[32] Lancaster JR Jr. A tutorial on the diffusibility and reactivity of free nitric oxide. Nitric Oxide 1997;1:18–30.

[33] Figueroa FE, Carrión F, Villanueva S, Khour M. Mesenchymal stem cell treatment for autoimmune diseases: a critical review. Biol Res 2012;45:269–77.

[34] Szabó E, Fajka-Boja R, Kriston-Pál É, Hornung Á, Makra I, Kudlik G, et al. Licensing by inflammatory cytokines abolishes heterogeneity of immunosuppressive function of

mesenchymal stem cell population. Stem Cells Dev 2015;doi:10.1089/scd.2014.0581.

[35] Novák J, Kriston-Pál É, Czibula Á, Deák M, Kovács L, Monostori É, et al. GM1 controlled lateral segregation of tyrosine kinase Lck predispose T-cells to cell-derived galectin-1-induced apoptosis. Mol Immunol 2014;57:302–9.

[36] Perone MJ, Bertera S, Tawadrous ZS, Shufesky WJ, Piganelli JD, Baum LG, et al. Dendritic cells expressing transgenic galectin-1 delay onset of autoimmune diabetes in mice. J Immunol 2006;177:5278–89.

[37] Hegyi B, Környei Z, Ferenczi S, Fekete R, Kudlik G, Kovács KJ, et al. Regulation of mouse microglia activation and effector functions by bone marrow-derived mesenchymal stem cells. Stem Cells Dev 2014;23:2600–12.

Appendix: Supplementary material

Supplementary data to this article can be found online at doi:10.1016/j.jcyt.2015.12.004.